

## Molecular-dynamics modeling of the Hugoniot of shocked liquid deuterium

Thomas J. Lenosky, Joel D. Kress,\* and Lee A. Collins

*Theoretical Division, Los Alamos National Laboratory, Los Alamos, New Mexico 87545*

(Received 11 March 1997)

Using our previously developed hydrogen tight-binding model, we performed equilibrium molecular-dynamics simulations to obtain the internal energy and pressure of the deuterium fluid at 39 separate (density, temperature) points. Our simulations are thought to represent the energetics of fluid hydrogen accurately, including molecular dissociation. We fit the thermodynamically-consistent simulation data with a virial expansion, obtaining a high-quality equation of state (EOS) fit. The fitting data span the ranges  $0.58 < \rho_D < 1.47$  g/cm<sup>3</sup> and  $3000 < T < 31\,250$  K, and the deduced EOS is thought to have a similar range of reliability. Our Hugoniot for shocked liquid deuterium shows a sharp rise in pressure and temperature at around 0.65–0.70 g/cm<sup>3</sup>. We compare our theoretical Hugoniot to recent experimental and theoretical results. [S0163-1829(97)06833-1]

### I. INTRODUCTION

Various experiments have probed the effect of a strong shock on liquid hydrogen or deuterium.<sup>1–4</sup> In recent experiments, single-shock pressures of up to 23 GPa have been reached for deuterium using a two-stage gas gun,<sup>3</sup> corresponding to a density of around 0.58 g/cm<sup>3</sup>, over three times greater than the liquid, and a temperature of around 4500 K. Previous gas-gun experiments had attained single-shock pressures of around 20 GPa (Ref. 1) and 21 GPa (Ref. 2). Multiple shocks with much higher pressures and densities were also produced in all of the gas-gun experiments. These pressures have reached a range between 80 and 180 GPa at temperatures of between 2000–5000 K. The derived densities of nearly 1 g/cm<sup>3</sup> or  $r_s \sim 1.4$  ( $r_s = a_i/a_B$  with  $a_i$  the ion-sphere radius) correspond to almost a factor of 10 compression of the initial liquid. Another recent experiment<sup>4</sup> used a high-energy pulse from the Nova laser to create an initial shock wave, which then propagated into a liquid deuterium sample chamber. It produced one single-shock datum at around 25 GPa and 5 single-shock data points at 70–210 GPa pressure, with inferred densities of over 1.0 g/cm<sup>3</sup>. These laser measurements have cast doubts on the standard deuterium equation of state (EOS) since, for a given pressure, the Nova densities range up to 50% higher than conventional EOS predictions, such as SESAME.<sup>5</sup>

The behavior of hot, dense hydrogen has importance within a diverse set of fields including astro-, plasma, condensed matter, and atomic and molecular physics. The understanding of the interiors of the gas giant planets<sup>6</sup> depends on a detailed knowledge of the EOS for hydrogen at moderate temperatures and high compressions. An analysis of shocked hydrogen also has direct technological importance, since the isotopic hydrogen fuel within a cryogenically cooled inertial confinement fusion (ICF) capsule may receive an initial strong shock,<sup>7</sup> well within the regime of our study.

Several previous hydrogen EOS models have been proposed.<sup>8,3,5</sup> The SESAME deuterium EOS was developed<sup>5</sup> by analytically modeling a number of physically important processes that occur in the hot, dense fluid. Thermodynamic contributions due to molecular interaction, rotation, vibra-

tion, dissociation, and ionization were included. At higher temperatures, both Thomas-Fermi-Dirac and Saha theories were used to provide a physically reasonable treatment of the ionized fluid.

A variety of direct simulation methods have been developed in recent years to treat hydrogen and other systems in this regime. The most sophisticated include the path-integral Monte Carlo<sup>9</sup> (PIMC) and the *ab initio* molecular dynamics (AIMD) for either the Car-Parrinello<sup>10</sup> or the explicit diagonalization prescriptions<sup>11</sup> within the local density approximation (LDA) density functional scheme. The computational intensity of these methods confines sample sizes and simulation times to fairly small values. In order to increase both, more approximate methods such as Thomas-Fermi<sup>12</sup> and tight-binding (TB) molecular dynamics<sup>13,14</sup> have evolved. The latter includes direct, exchange, and correlation electronic effects although in a less explicit fashion than the PIMC and AIMD approaches. By choosing the TB matrix elements to reproduce known properties, we have fit a TB model<sup>13</sup> that accurately represents molecular vibrations, rotation, and dissociation, including interactions among separate molecules and dissociated atoms. The model also includes ionization in an approximate way, correct to the extent that single atomic orbitals can be superposed to represent lower-lying excited states. These processes occur naturally and simultaneously during a molecular-dynamics simulation, so that synergistic effects (e.g., rotational-vibrational couplings) are taken into account as a matter of course.

In recent work,<sup>13</sup> we applied this tight-binding model to the understanding of electrical conductivity in shocked hydrogen. Recent multiple-shock gas-gun experiments<sup>3,15</sup> reached high compressions at fairly low temperatures. Measurements indicated<sup>15</sup> a rapid rise in electrical conductivity, as the density increases. To examine this, we performed molecular dynamics simulations, and then obtained electrical conductivities using a Mott formula.<sup>16</sup> The calculated values had a similar magnitude to the experimental observations ( $\sigma \sim 2000 \Omega^{-1} \text{cm}^{-1}$ ), and also showed a strong increase with increasing temperature or density. The mechanism for the conductivity was identified to be electron hopping among

TABLE I. Parameters that specify the optimized tight-binding potential. The model is determined by the three functions  $\phi(r)$ ,  $h_{ss\sigma}(r)$ , and  $s_{ss\sigma}(r)$ . We have defined the functions  $g_{ss\sigma}(r)$  and  $f_{ss\sigma}(r)$ , by  $h_{ss\sigma}(r) = (1/r^2)g_{ss\sigma}(r)$ , and  $s_{ss\sigma}(r) = (1/r^2)f_{ss\sigma}(r)$ . The functions  $g_{ss\sigma}(r)$ ,  $f_{ss\sigma}(r)$ , and  $\phi(r)$  are represented as cubic splines that go smoothly to zero at  $r_u = 6.8 a_B$ . Each function is defined only for interatomic distances greater than  $r_l = 0.5 a_B$ . The functions have six spline knots between  $r_l$  and the upper end point  $r_u$ . The upper portion of the table gives the values of the functions at these knots, while the lower portion contains the first derivative of each function at the end points. All quantities are expressed using energy units of Rydberg, and distance units of bohr.

$r$	$\phi(r)$	$g_{ss\sigma}(r)$	$f_{ss\sigma}(r)$
0.5	1.03538	-0.27368	0.24553
1.4	0.07026	-1.49207	0.90707
2.3	0.00338	-2.44663	1.62375
3.2	0.00441	-2.33403	1.69573
4.1	0.00182	-1.83574	1.49678
5.0	-0.00104	-0.98518	0.93742
5.9	-0.00031	-0.39800	0.52277
6.8	0.00000	0.00000	0.00000
$r$	$(\phi(r))'$	$(g_{ss\sigma}(r))'$	$(f_{ss\sigma}(r))'$
0.5	-2.45223	-0.83539	0.01377
6.8	0.00000	0.00000	0.00000

dissociated atoms, as previously proposed by Ross.<sup>17</sup> The success of our model in explaining the conductivity of H has encouraged us to generate a full EOS in this regime.

## II. FITTING A TIGHT-BINDING MODEL

We previously developed a new TB model<sup>13</sup> that accurately represents hydrogen in the realm of the shock experiments and that merges with the results of our older TB model<sup>14</sup> at higher temperatures and pressures. Our fitting methodology followed that used for silicon.<sup>18</sup> The total TB energy has the form

$$E = \sum_i f_i \epsilon_i + \sum_{i < j} \phi(R_{ij}), \quad (1)$$

where  $f_i$  is the occupation number based on a Fermi-Dirac distribution at temperature  $T$ ,  $\phi$  is an effective pair potential,  $\epsilon_i$  is an eigenvalue of  $H\psi_i = \epsilon_i S\psi_i$ ,  $H$  and  $S$  are the Hamiltonian and overlap matrices, respectively, and  $R_{ij}$  is the distance between atoms  $i$  and  $j$ . Only a single  $s$ -type orbital occupies each atomic center in this model. We performed nonlinear least-squares fits to find the optimal form of the functions,  $\phi(r)$ ,  $h_{ss\sigma}(r)$ , and  $s_{ss\sigma}(r)$ , which represent the pair potential, and the two-center matrix elements of the Hamiltonian and overlap matrices, respectively. We represented these functions using cubic splines, which go smoothly to zero at a 6.8 bohr cutoff. The parameters given in Table I were chosen to best reproduce a set of *ab initio* results. The zero of energy was chosen so that a free, charge-neutral, atom would have energy  $-1$  Ry.

These *ab initio* results include (1) the ground and antibonding electronic states of  $H_2$  as a function of nuclear

separation;<sup>14</sup> (2) the zero-temperature pressure at five densities ( $r_s = 1.6 - 2.2$ ) of molecular hydrogen;<sup>19-21</sup> (3) the simple-cubic (sc) and body-centered-cubic (bcc) atomic crystal energies as a function of lattice constant;<sup>22</sup> and (4) atomic forces from an LDA molecular-dynamics simulation for 54 atoms at  $r_s = 2$  and  $T = 15\,780$  K at several configurations.<sup>23</sup> In general, we obtained a good fit to this data. Most importantly, our model accurately predicts the energy of the ground and antibonding electronic states of  $H_2$ , with a global error of less than 0.007 and 0.02 Ry/atom, respectively. The sc and bcc atomic structures were given a lesser weight in our fit. We overestimate these energies by up to 0.012 and 0.04 Ry/atom, respectively, although as for  $H_2$ , typical errors are somewhat smaller. The magnitude of all these errors can be better appreciated by noting that 0.01 Ry corresponds to a temperature of only about 1600 K.

As a test of the predictive quality of the model, we considered cases not included in the fit. For example, for the high-coordination face-centered-cubic (fcc) structure, we overestimated the LDA results<sup>22,24</sup> by up to 0.02 Ry/atom, and the low-coordination primitive hexagonal and diamond phases yielded energies lower by about 0.03 Ry/atom relative to quantum Monte Carlo (QMC) results.<sup>25</sup> There are significant discrepancies in reported molecular solid pressures between LDA,<sup>20</sup> QMC,<sup>19</sup> and experiment.<sup>21</sup> We fit primarily to the experimental pressure values. The other *ab initio* energies used in fitting may plausibly contain error on the order of 0.01 Ry/atom, except for the hydrogen molecule electronic states, which should be considerably more accurate. We also did not attempt to directly model nuclear zero-point energy, which should represent around 0.01 Ry/atom under the conditions of this study.

## III. MOLECULAR-DYNAMICS SIMULATION

Using our model, constant-volume molecular-dynamics simulations were performed at various densities and temperatures. We used the Verlet algorithm for integrating the equations of motion and maintained constant temperature in the isokinetic ensemble by velocity scaling. The electronic temperature was set using a Fermi-Dirac distribution with the Fermi temperature  $T_F$  always set equal to the ionic temperature  $T$ . Electronic states were computed at only the  $\Gamma$  point in reciprocal space. These aspects of the calculation were identical to Refs. 11 and 14. Fluid pressure  $P$  was computed for each constant-volume simulation, as discussed in Ref. 26, using the Hellmann-Feynman forces as input.<sup>27</sup> The internal energy per atom  $U$  was computed using the nuclear kinetic energy and the time average of the tight-binding energy  $E$ , Eq. (1):

$$U = \frac{3}{2} k_B T + \frac{E}{N}. \quad (2)$$

[In a previous paper<sup>13</sup> we defined the internal energy per atom  $U$  as not including the nuclear kinetic energy, and denoted it as  $U/N$  rather than  $U$ . For convenience, we also now are defining  $U$  as an intensive (per atom) quantity, rather than an extensive quantity.] We used a short time step of

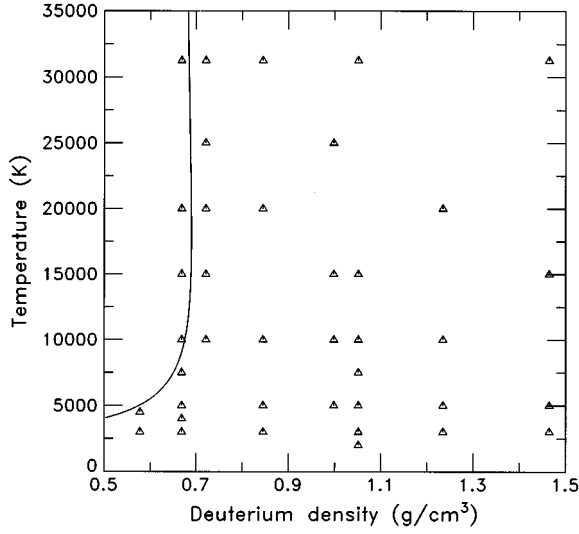


FIG. 1. Calculated Hugoniot temperature vs deuterium density (solid line) for our EOS. Triangles represent density and temperature conditions of the 39 molecular-dynamics simulations used in our fitting.

0.2 fs, and a cubic periodic cell, typically with 250 atoms, in each case allowing the hydrogen to reach full equilibrium before collecting statistics for 3000–4000 time steps. The simulations always reached complete equilibrium within several hundred fs, regardless of initial conditions.

We performed a number of careful tests of our simulation code.<sup>13</sup> Most importantly, the tight-binding energetics were tested and found to be in complete agreement with an independent tight-binding code. All of our final simulations had 250 atoms per unit cell. We also performed some test simulations with 54, 128, and 432 atoms per cell.<sup>13</sup> In these tests, very little size dependence was found in  $P$  or  $U$ , although  $P$  was a somewhat more sensitive quantity. We conservatively estimate that simulation errors in  $P$ , due to fixing the number of atoms at 250, should be less than 1%. Statistical errors due to finite simulation length appear to be of a roughly similar magnitude,<sup>13</sup> again with  $P$  being more difficult to determine accurately than  $U$ . However, such statistical errors are less important than systematic errors in the context of EOS fitting, because they can be partially averaged during the fitting process.

We performed 39 molecular-dynamics simulations at different densities and temperatures (see Fig. 1) to obtain a table for fitting our EOS. The simulation points were chosen to span a range of densities and temperatures, with greatest coverage in regions of greatest interest. Our EOS fitting methodology does not require a regular grid of points. We found it useful, however, to perform simulations in a somewhat regular manner. For example, at  $r_s=2.0$  ( $\rho_D=0.67$  g/cm<sup>3</sup>) we performed simulations at 8 different temperatures, in order to obtain an accurate temperature dependence of the EOS at that fixed density.

#### IV. FITTING A SMOOTH EQUATION OF STATE

Given the results of the molecular-dynamics simulations, we fit smooth functions for the fluid pressure  $P$ , and internal energy per atom  $U$ :

TABLE II. EOS coefficients  $c_{ij}$ , expressing fluid pressure  $P$  as a function of density and temperature.

$i$	$j$	$c_{ij}$
2	0	$-4.633864 \times 10^4$
3	0	$1.675689 \times 10^6$
4	0	$-9.837730 \times 10^6$
1	1	$1.354806 \times 10^{-1}$
2	-1	$1.079888 \times 10^8$
3	-1	$-1.250218 \times 10^9$
2	-2	$-4.907503 \times 10^{10}$

$$P = \sum_{ij} c_{ij} n^i T^j, \quad (3)$$

$$U = \sum_{ij} d_{ij} n^i T^j, \quad (4)$$

where  $n=N/V$  is the number of atoms per unit volume (expressed in  $a_B^{-3}$ ) and  $T$  is the temperature (in Kelvin), with  $P$  and  $U$  given in GPa and Ry/atom, respectively. The 17 EOS coefficients  $c_{ij}$  and  $d_{ij}$  are given in Table II and Table III. They were chosen so that  $P$  and  $U$  would be thermodynamically consistent:

$$P - T \left( \frac{\partial P}{\partial T} \right)_V = - \left( \frac{\partial U}{\partial V} \right)_T. \quad (5)$$

This well-known condition follows directly from a Maxwell relation of the Helmholtz free energy  $F=U-TS$ . Because of it, only 11 of the 17 fitting coefficients are independent variables. Our input table of molecular-dynamics simulation data is itself thermodynamically consistent, except for very small statistical simulation errors. This is guaranteed because we used exact formulas for calculating  $U$  and  $P$ , and each simulation was conducted in a nearly identical manner. For example, we did not vary the number of atoms (250), or the cubic shape of the simulation cell. Any nonequilibrium in the simulations would probably have resulted in thermodynamic inconsistency, which would have become evident during EOS fitting. In this way, the thermodynamic consistency of our data provides additional evidence that our simulations were properly equilibrated.

TABLE III. EOS coefficients  $d_{ij}$ , expressing internal energy  $U$  [Eq. (2)] as a function of density and temperature.

$i$	$j$	$d_{ij}$
0	0	$-1.076424 \times 10^0$
1	0	$-3.149982 \times 10^0$
2	0	$5.695452 \times 10^1$
3	0	$-2.229146 \times 10^2$
0	-1	$-4.980893 \times 10^2$
1	-1	$1.468161 \times 10^4$
2	-1	$-8.498664 \times 10^4$
0	-2	$4.190578 \times 10^5$
1	-2	$-1.000798 \times 10^7$
0	1	$1.310923 \times 10^{-5}$

The EOS coefficients were obtained by nonlinear least-squares fitting, which included all of the pressure and internal energy data simultaneously. We weighted the pressure data in fitting, so that a given percentage error in any pressure would be equally undesirable. The weight of each internal energy value in the fit was a constant multiplied by the weight for the corresponding pressure. This single constant was chosen so that energy and pressure data would have roughly equal overall contributions to the fit. We felt this weighting scheme made the best use of all the available data, although other reasonable weighting schemes gave almost identical fits.

The average error our model made in predicting  $U$  for the 39 data points was 0.00132 Ry/atom, and the average error in predicting  $P$  was 1.06 GPa. The average percentage error for  $P$  was 1.17%. This error is comparable to the statistical simulation error in the original simulation data, which we judge to be about 1%. The worst errors in  $U$  and  $P$  were 0.01023 Ry/atom and 3.49 GPa, with a worst percentage error in  $P$  of 4.02%. These larger errors may be due in part to statistical outliers in the fitting data; no unusually large errors occur directly around our calculated Hugoniot curve.

We chose the smallest set of fitting terms  $c_{ij}n^iT^j$  and  $d_{ij}n^iT^j$ , which gave a high-quality fit. The form of our present EOS is quite similar to the virial expansion for the properties of an ordinary gas. The  $T^{-1}$  and  $T^{-2}$  temperature dependence of some of the terms in the current model arises naturally<sup>28</sup> when the partition function of a fluid is expanded in powers of  $\beta=1/k_B T$ . Fitting with exclusively non-negative powers  $j$  of  $T$  gave a somewhat poorer fit, and required more terms.

The quality and simplicity of our final fit, together with the occurrence of only small powers of  $n$  and  $T$ , gives us confidence that the EOS will be reliable over the range of the fitting data, about  $0.58 < \rho_D < 1.47$  g/cm<sup>3</sup> and  $3000 < T < 31250$  K. Outside this range the quality of the EOS becomes poor. This is especially true at lower temperatures, as the  $T^{-1}$  and  $T^{-2}$  terms dominate. Our EOS is smooth and essentially featureless, showing no evidence for a phase transition within its region of applicability. In particular  $\partial P/\partial T$  is positive everywhere; we do not see the negative  $\partial P/\partial T$  values cited as evidence for a phase transition within PIMC.<sup>9</sup> Our work also provides no evidence for the plasma phase transition that appears in the models of Saumon and Chabrier<sup>29</sup> and Reinholz *et al.*<sup>30</sup>

## V. CALCULATING THE HUGONIOT

The Rankine-Hugoniot equation<sup>31</sup> gives the shock adiabat, given an initial volume  $V_1$ , internal energy  $U_1$ , and pressure  $P_1$ :

$$(U_1 - U_2) + \frac{1}{2}(V_1 - V_2)(P_1 + P_2) = 0. \quad (6)$$

The shock adiabat is the set of final conditions with volume  $V_2$ , pressure  $P_2$ , and internal energy  $U_2$ , that satisfy this equation. We solved Eq. (6) numerically, using our EOS for  $P_2$  and  $U_2$  at each volume  $V_2$ . Equation (6) represents conservation of mass, energy, and momentum at the shock front, hence it is quite general.

The initial state was taken to be liquid deuterium with a volume  $V_1 = 23.5$  cm<sup>3</sup>/mol, which corresponds to a density

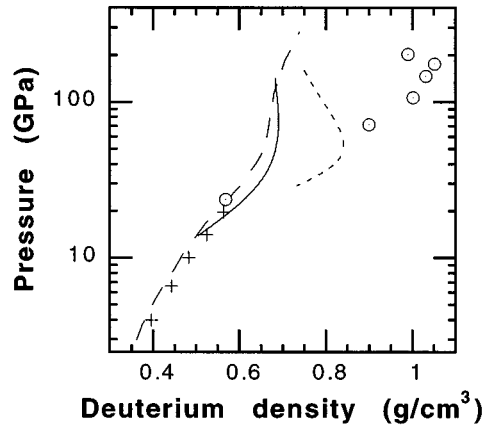


FIG. 2. Single-shock Hugoniot curves calculated using our EOS (solid line) and the SESAME library EOS (longer dashed line). Circles represent data points from the Nova laser experiment, while crosses are the result of gas-gun experiments. Initial condition is cryogenic liquid deuterium in each study. Shorter dashed line shows sensitivity of our Hugoniot prediction to an *ad hoc* 1-eV/atom shift in the internal energy.

of  $\rho_D = 0.171$  g/cm<sup>3</sup>. This value is typical of experimental conditions.<sup>2-4</sup> We ignore the very small initial pressure  $P_1$ , setting  $P_1 = 0$ . The initial internal energy  $U_1$  was not obtained directly from our EOS [Eq. (4)], which is not valid at such low densities. Our tight-binding model predicts a binding energy of  $-1.1691$  Ry/atom for the isolated hydrogen molecule. (The energy of the low-density liquid would be nearly identical.) We found it reasonable to adjust this value by 0.020 Ry/atom to improve agreement of our Hugoniot with gas-gun shock data,<sup>2</sup> setting  $U_1 = -1.1491$  Ry/atom. This optimizes agreement with the two highest-pressure gas-gun data points (see Fig. 2), which actually lie slightly below the range of our original fitting data. The correction mainly serves to subtract away low-density errors in our tight-binding model, which was fit using no data at densities below  $\rho_D = 0.50$  g/cm<sup>3</sup> ( $r_s = 2.2$ ). As we discuss at greater length below, the Hugoniot becomes insensitive to small variations in  $U$ , as the temperature, and hence the energy scale, rises.

## VI. DISCUSSION

Our calculated Hugoniot (Fig. 1 and Fig. 2) is very similar to that calculated with SESAME.<sup>5</sup> We predict densities up to 7% higher than SESAME, an amount that might be expected, given the approximations inherent in each model. The five highest pressure measurements from Nova<sup>4</sup> differ from these calculations by up to 50% in density. In Fig. 2, we did not reproduce the original error bars on the Nova data, which allow for only about one-quarter of this discrepancy. In both figures, our calculated Hugoniot stops at 35000 K to reflect the range of validity of the EOS. The Nova data are completely within its range, because at higher densities the EOS extends to higher pressures.

We wanted to understand the large discrepancy between the Nova data and our results. In general, absorption of energy in a medium will result in higher shock-compression densities. Holmes, Ross, and Nellis<sup>3</sup> recently proposed a

model in which molecular dissociation plays such a role. While dissociation of a hydrogen molecule in free space requires 2.2 eV/atom, this value should be greatly reduced within a high-density fluid, because the dissociated atoms remain closely associated with other atoms and molecules. The energy difference between (completely dissociated) atomic<sup>22,24,25</sup> and molecular<sup>20,19</sup> crystal phases, less than 1 eV/atom, should set an upper bound on the contribution of dissociation to the internal energy  $U$  of the fluid.

We expect our tight-binding model would accurately recover any dissociation energy, especially given that such crystal phases were used in fitting. To examine the sensitivity of our Hugoniot to any errors, in Fig. 2 we show the Hugoniot resulting from shifting our EOS function  $U$  [Eq. (4)] by adding 1 eV/atom. [We did not try shifting  $P$  in unison, because it would only tend to increase, counterbalancing to some extent the shift in  $U$  in Eq. (6). This might reduce the sensitivity to error by an additional factor of 2 or more.] The effect of this shift is quite significant, yet it does not suffice to generate good agreement with the four highest-pressure Nova measurements. Roughly 3 to 5 eV/atom corrections in  $U$  are necessary to generate such agreement. Rather large shifts are needed because the Hugoniot becomes less sensitive to shifts in  $U$  at higher temperatures, as the energy scale of the problem increases.

Our Hugoniot prediction was surprisingly insensitive to the amount of EOS fitting data, or the method used in fitting the EOS. At the time of our earliest fits, we had performed only 11 of the 39 final molecular-dynamics simulations. Fitting an EOS to these in a very crude fashion yielded a Hugoniot quite similar to our final prediction, with predicted densities within about 5% for pressures of 30 to 100 GPa. Varying the weighting scheme for the data, or the terms kept in Eqs. (3) and (4), generally resulted in much smaller effects. Density changes along the Hugoniot were never more than 2–3%, even for poor fits to the simulation data. Also, late in the study, many of the fitting data at  $r_s = 2.0$  and 1.95 ( $\rho_D = 0.67$  and  $0.72$  g/cm<sup>3</sup>) were added, to constrain the Hugoniot somewhat more accurately. The insensitivity that we observed during the fitting process is clearly another aspect of the numerical stability of the Hugoniot to perturbations in the EOS.

## VII. CONCLUSION

In this work, we have studied the response of cryogenic liquid deuterium to strong shock waves under the assumption of thermodynamic equilibrium. This was done using a tight-binding model that accurately represents the interactions among deuterium atoms and molecules, including molecular

vibrations and rotations, dissociation, and ionization. Our model was previously applied in a study of electrical conductivity.<sup>13</sup> Using this model, we performed 39 molecular-dynamics simulations at various densities and temperatures. Using these simulation points, we fit a smooth EOS describing the internal energy and fluid pressure over the range  $0.58 < \rho_D < 1.47$  g/cm<sup>3</sup> and  $3000 < T < 31\,250$  K. Our thermodynamically consistent EOS has the form of a virial expansion containing only 11 independent fitting parameters. It is smooth and well behaved, showing no evidence for any phase transition.

Using our EOS fit, we constructed the Hugoniot of shocked liquid deuterium. We used a typical experimental value for the liquid density, and adjusted our tight-binding internal energy slightly to improve the agreement of our Hugoniot with experimental gas-gun measurements. This was justified because neither our tight-binding model nor our EOS were fit for such low fluid densities. Within the region of validity of our EOS, our calculated Hugoniot is remarkably similar to the previous SESAME library EOS,<sup>5</sup> although our prediction reaches densities a few percent higher.

We considered the results of a recent Nova laser experiment,<sup>4</sup> which found single-shock densities of around 1.0 g/cm<sup>3</sup> at pressures of 100–200 GPa. These density values are about 50% higher than predicted by our EOS or the SESAME EOS. This excursion to higher densities was previously attributed to energy absorption due to molecular dissociation.<sup>4</sup> We examined the effect of an *ad hoc* adjustment in our EOS internal energy on the Hugoniot. A 3 to 5 eV/atom shift in energy was needed to obtain good agreement with the Nova data. This energy shift is too large to possibly be produced by molecular dissociation, since the binding energy of a D<sub>2</sub> molecule in free space is only about 2.2 eV/atom. We also expect that our modeling already represents molecular dissociation in an accurate way, so that any large correction due to dissociation is not plausible. Our Hugoniot analysis, based on the experimental claims, assumes that the material has reached thermodynamical equilibrium. Violation of this condition could account for a major source of disagreement. In this case, however, the experiment would no longer measure a Hugoniot.

## ACKNOWLEDGMENTS

We would especially like to thank J. D. Johnson for very helpful discussions, and also for his comments on this manuscript. We also wish to thank Ard Louis, William Magro, William Nellis, L. Da Silva, Norm Troullier, Arthur Voter, and Jing Zhu.

\* Author to whom correspondence should be addressed.

<sup>1</sup>A. H. Jones, W. M. Isbell, and C. J. Maiden, *J. Appl. Phys.* **37**, 3493 (1966); M. van Thiel, M. Ross, B. L. Hord, A. C. Mitchell, W. H. Gust, M. J. D'Addario, and R. N. Keeler, *Phys. Rev. Lett.* **31**, 979 (1973); M. van Thiel, L. B. Hord, W. H. Gust, A. C. Mitchell, M. D'Addario, K. Boutwell, E. Wilbarger, and B. Barrett, *Phys. Earth Planet. Inter.* **9**, 57 (1974).

<sup>2</sup>W. J. Nellis, A. C. Mitchell, M. van Thiel, G. J. Devine, R. J. Trainor, and N. Brown, *J. Chem. Phys.* **79**, 1480 (1983).

<sup>3</sup>N. C. Holmes, M. Ross, and W. J. Nellis, *Phys. Rev. B* **52**, 15 835 (1995).

<sup>4</sup>L. B. DaSilva, P. Celliers, G. W. Collins, K. S. Budil, N. C. Holmes, T. W. Barbee, Jr., B. A. Hammel, J. D. Kilkenny, R. J. Wallace, M. Ross, R. Cauble, A. Ng, and G. Chiu, *Phys. Rev. Lett.* **78**, 483 (1997).

<sup>5</sup>G. I. Kerley, in *Molecular-Based Study of Fluids*, edited by J. M. Haile and G. A. Mansoori (American Chemical Society, Washington, DC, 1983), pp. 107–138.

- <sup>6</sup>W. J. Nellis, S. T. Weir, and A. C. Mitchell, *Science* **273**, 936 (1996).
- <sup>7</sup>J. D. Lindl, R. L. McCoy, and E. M. Campbell, *Phys. Today* **45** (9), 32 (1992).
- <sup>8</sup>D. Saumon and G. Chabrier, *Phys. Rev. A* **44**, 5122 (1991); D. Saumon, W. B. Hubbard, G. Chabrier, and H. M. van Horn, *Astrophys. J.* **391**, 827 (1992).
- <sup>9</sup>W. R. Magro, D. M. Ceperley, C. Pierleoni, and B. Bernu, *Phys. Rev. Lett.* **76**, 1240 (1996); C. Pierleoni, D. M. Ceperley, B. Bernu, and W. R. Magro, *Phys. Rev. Lett.* **73**, 2145 (1994).
- <sup>10</sup>D. Hohl, V. Natoli, D. M. Ceperley, and R. M. Martin, *Phys. Rev. Lett.* **71**, 541 (1993); J. Kohanoff and J-P. Hansen, *Phys. Rev. E* **54**, 768 (1995).
- <sup>11</sup>L. Collins, I. Kwon, J. Kress, N. Troullier, and D. Lynch, *Phys. Rev. E* **52**, 6202 (1995).
- <sup>12</sup>J. I. Penman, J. G. Clerouin, and P. G. Zerah, *Phys. Rev. E* **51**, R5224 (1994).
- <sup>13</sup>T. J. Lenosky, J. D. Kress, L. A. Collins, and I. Kwon, *J. Quant. Spectrosc. Radiat. Transfer* (to be published); *Phys. Rev. B* **55**, R11 907 (1997).
- <sup>14</sup>I. Kwon, J. D. Kress, and L. A. Collins, *Phys. Rev. B* **50**, 9118 (1994).
- <sup>15</sup>S. T. Weir, A. C. Mitchell, and W. J. Nellis, *Phys. Rev. Lett.* **76**, 1860 (1996).
- <sup>16</sup>N. F. Mott and E. A. Davis, *Electronic Processes in Non-Crystalline Materials* (Clarendon Press, Oxford, 1979), Chap. 1.
- <sup>17</sup>M. Ross, *Phys. Rev. B* **54**, R9589 (1996).
- <sup>18</sup>T. J. Lenosky, J. D. Kress, I. Kwon, A. F. Voter, B. Edwards, D. F. Richards, S. Yang, and J. B. Adams, *Phys. Rev. B* **55**, 1528 (1997).
- <sup>19</sup>D. M. Ceperley and B. J. Alder, *Phys. Rev. B* **36**, 2092 (1987).
- <sup>20</sup>B. I. Min, H. J. F. Jansen, and A. J. Freeman, *Phys. Rev. B* **33**, 6383 (1986).
- <sup>21</sup>P. Loubeyre, R. LeToullec, D. Hausermann, M. Hanfland, R. J. Hemley, H. K. Mao, and L. W. Finger, *Nature (London)* **383**, 702 (1996); H. K. Mao and R. J. Hemley, *Rev. Mod. Phys.* **66**, 671 (1994); R. J. Hemley, H. K. Mao, L. W. Finger, A. P. Jephcoat, R. M. Hazen, and C. S. Zha, *Phys. Rev. B* **42**, 6458 (1990); J. van Straaten and I. F. Silvera, *ibid.* **37**, 1989 (1988).
- <sup>22</sup>B. I. Min, H. J. F. Jansen, and A. J. Freeman, *Phys. Rev. B* **30**, 5076 (1984).
- <sup>23</sup>I. Kwon, L. Collins, J. Kress, and N. Troullier, *Phys. Rev. E* **54**, 2844 (1996).
- <sup>24</sup>T. W. Barbee III and M. L. Cohen, *Phys. Rev. B* **44**, 11 563 (1991).
- <sup>25</sup>V. Natoli, R. M. Martin, and D. M. Ceperley, *Phys. Rev. Lett.* **70**, 1952 (1993).
- <sup>26</sup>M. P. Allen and D. J. Tildesley, *Computer Simulations of Liquids* (Clarendon Press, Oxford, 1987).
- <sup>27</sup>O. F. Sankey and R. E. Allen, *Phys. Rev. B* **33**, 7164 (1986).
- <sup>28</sup>F. Reif, *Fundamentals of Statistical and Thermal Physics* (McGraw-Hill, New York, 1965).
- <sup>29</sup>D. Saumon and G. Chabrier, *Phys. Rev. Lett.* **62**, 2397 (1989).
- <sup>30</sup>H. Reinholz, R. Redmer, and S. Nagel, *Phys. Rev. E* **52**, 5368 (1995).
- <sup>31</sup>L. D. Landau and E. M. Lifshitz, *Fluid Mechanics*, 2nd ed. (Pergamon Press, Oxford, 1987).